

# Investigation of Defect Cavities Formed in Inverse Three-Dimensional Rod-Connected Diamond Photonic Crystals

Mike P.C. Taverne, Lifeng Chen, Xu Zheng, Martin Lopez-Garcia, Ying-Lung D. Ho, and John G. Rarity  
 Department of Electrical and Electronic Engineering, University of Bristol  
 Merchant Venturers Building, Woodland Road  
 Bristol BS8 1UB, UK

**Abstract-** We report the optical properties of single defects in inverse three-dimensional (3D) rod-connected diamond (RCD) photonic crystal (PhC) cavities by using plane-wave expansion (PWE) and finite-difference time domain (FDTD) methods. By optimizing the dimensions of a 3D inverse RCD PhC, wide photonic band gaps (PBG) are obtained. Optical cavities with resonances in the bandgap arise when point defects are introduced in the crystal. A variety of shapes and locations of single defects are investigated in high-refractive-index contrast (gallium phosphide-air or chalcogenide-air) inverse RCD structures, and  $Q$ -factors and mode volumes ( $V_{eff}$ ) of the resonant cavity modes are calculated. By choosing a single sphere defect located at the center of a tetrahedral arrangement, small mode volumes can be obtained. Here, high  $Q$ -factors up to 724,000 and cavity mode volumes down to  $V_{eff} < 0.3(\lambda/n)^3$  have been demonstrated.

## I. INTRODUCTION

An atomic crystal forms from a periodic and systematic arrangement of atoms within which electrons feel a periodic potential. This leads to, wavevector specific electronic bandstructures and is the origin of electronic bandgaps in semiconductor materials. Similarly, in a photonic crystal, the dielectric function varies periodically, leading to photonic band structures. In the same way that localized electron states can be created within atomic crystal lattices by introducing defects, photons can be confined within defects in dielectric crystal lattices [1].

Various three-dimensional (3D) photonic crystal (PhC) structures with complete PBGs have been fabricated using two-photon polymerization (2PP) based 3D lithography by direct laser writing (DLW) with or without backfilling materials to create 3D high-refractive-index-contrast nanostructures [2]. We are actively pursuing 3D fabrication of such structures using DLW and have already seen partial bandgaps in 3D photonic crystals at 1550 nm [3].

Photonic diamond lattice structures such as rod-connected diamond (RCD) [4,5], are known to exhibit the largest full PBG [6]. Such structures have been numerically investigated using the plane-wave expansion (PWE) [7] method and finite-difference time domain (FDTD) calculations [8]. In this work, we investigate the potential to create high- $Q$  low mode volume cavities using the optical properties of single defects in 3D inverse RCD PhC cavities. Analysis using the PWE method has shown a full photonic bandgap in technically interesting wavelength regions. We have studied the optimization of

relative gap width (gap width to midgap frequency ratio) as a function of the rod width using MIT Photonic-Bands software (MPB) [9]. Our in-house FDTD software [10] is then used to calculate the time response and transmission spectrum of the finite inverse RCD crystal structures containing three types of single defect cavities (rod, block, and sphere) located at different unique positions along the [1,1,1] axis of the crystal. Here, we demonstrate high  $Q$ -factors up to 724,000, which is limited only by simulation volume constraints, and cavity mode volumes down to  $V_{eff} < 0.3(\lambda/n)^3$ . These results are comparable to our recent published paper [11] and other reported structures [12].

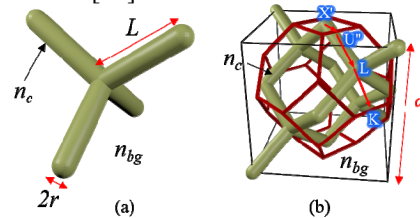


Fig. 1. (a) The main tetrahedral “building block” of the RCD structure. The rods, of diameter  $2r$  and length  $L$  are made of low refractive index material ( $n_c$ ) and surrounded by high-refractive-index material ( $n_{bg}$ ). (b) A cubic unit-cell of RCD of lattice constant  $a$  and the orientation of its Brillouin zone (in red) relative to it.

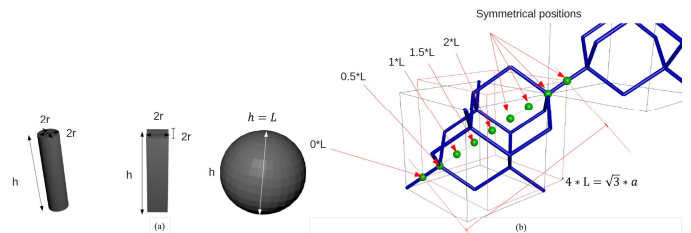


Fig. 2. (a) Three type of defect shapes. (b) Defect positions along the [1,1,1] axis.

## II. GEOMETRY AND BANDGAPS: 3D RCD PHOTONIC CRYSTAL CAVITY DESIGN

### A. Geometry: Design of the Model

We are studying the inverse RCD structure as shown in Fig. 1. The inverse RCD structure replaces the bonds in a diamond lattice with low-refractive-index rods surrounded by high-index material. This can be visualized as a non-primitive cubic unit cell in Fig. 1 (b), which contains 16 elliptical cylinders, which can be grouped into four regular tetrahedral arrangement like the one shown in Fig. 1(a).

For the defects, three shapes were considered: a cylinder, a block and a sphere. Their dimensions are detailed in Fig 2 (a). The defects are labeled Bn, Cn, Sn for block, cylinder and sphere respectively, where n corresponds to the location along the [1,1,1] axis as illustrated in Fig. 2 (b).

**B. Bandgaps: Photonic Bands of an Inverse 3D RCD PhC.**

We used the MIT photonic bands package, which solves the frequency domain eigenproblem for a periodic dielectric structure, giving us the allowed propagation modes for different wavevectors  $k$ . The results for the high-refractive-index contrast (gallium phosphide-air) inverse RCD structure described below using  $r/a = 0.26$ ,  $n_c = 1.0$ , and  $n_{bg} = 3.3$  are shown in Fig. 3(a). A full bandgap from  $a\lambda \in [0.5140, 0.6598]$  (midgap frequency  $a\lambda = 0.5869$ ) is clearly seen. Fig. 3(b) shows an optimal radius for each given index contrast (1:2.4, 1.52:3.3, 1:3.3).

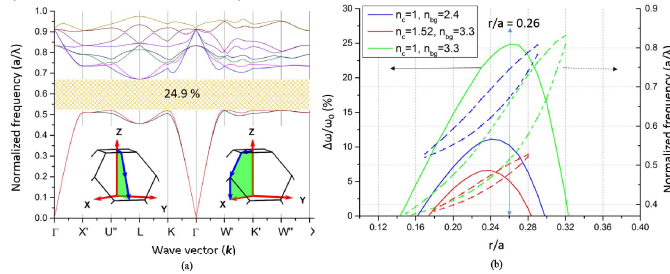


Fig. 3. (a) Bandgap diagram of an inverse RCD with rods of refractive index 1.0 (vacuum) and a backfill of refractive index 3.3, created with the MPB software. (b) Gap-midgap ratio  $\Delta\omega/\omega_0$  (between band 2 and band 3) (bold lines) and normalized frequency  $a/\lambda$  (dashed lines) as a function of  $r/a$ , where  $r$  is the radius of the inverse RCD rods and  $a$  is its lattice constant as explained in Fig. 1(b). There is an optimal radius for each given index contrast (1:2.4, 1.52:3.3, and 1:3.3).

**III. CALCULATING RELEVANT PARAMETERS OF THE DEFECT CAVITIES**

In the following, we show how we calculate relevant parameters for our cavity structures. These are the cavity resonant wavelength  $\lambda$ , quality factor  $Q$  and mode volume  $V_{eff}$ .

**A. Resonant Wavelength and Q-factors of Defect Cavities**

For each defect type, three FDTD simulations (one for each direction: X, Y, Z) were run using a broadband dipole source placed in the defect. The Q-factor can then be calculated by analyzing the resulting field decay in the frequency domain. The field decay and spectrum for an inverse RCD with a sphere defect ( $h = 2r$ ) are shown in Fig. 4 (a). A nonhomogeneous mesh of around  $10^7$  cells adapted to the geometry was used.

**B. Calculating the Effective Mode Volume  $V_{eff}$**

Having determined the resonant frequency, we can visualize a cavity mode on resonance using single frequency “snapshots.” We illustrate the confinement of the electric field energy density distribution in each plane,  $y-z$ ,  $x-z$ , and  $y-x$ , in Fig. 5 for a sphere defect located at the position  $0.5*L$  (i.e., the center of a tetrahedral arrangement). The field is strongly localized to the defect. We obtain the Q-factors and mode volumes of the cavity modes shown in Fig. 5(b) for the 9 considered defects.

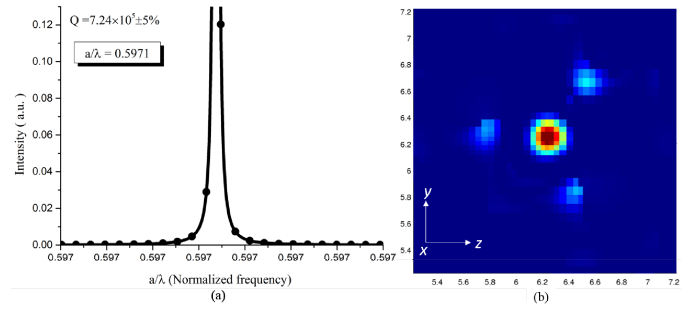


Fig. 4. (a) Fast Fourier transform of the field decay, near a sphere defect located at the position  $0.5*L$  (i.e., the center of a “tetrahedral arrangement”).  $n_{rod} = 1.0$  and  $n_{def} = n_{bg} = 3.3$  and a defect height (diameter)  $h = 2r$ . The X-dipole excites a resonance at  $a/\lambda = 0.5971$  with  $Q$ -factor  $7.24 \times 10^5$ . (b) A resonant frequency snapshot of the defect cavity mode energy density distribution  $\epsilon(|E_x|^2 + |E_y|^2 + |E_z|^2)$  in the central X plane.

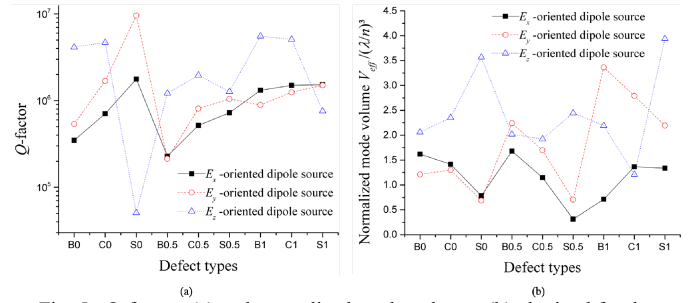


Fig. 5. Q-factors (a) and normalized mode volumes (b) obtained for the different defect types considered.

**IV. CONCLUSION**

We investigated various defects (rod, block, and sphere) located along the [1,1,1] axis of inverse RCD crystals. The preliminary corresponding results are shown in Fig. 4, Fig. 5 and Fig.6. The sphere defect gives the best results for an excitation in the  $E_x$  direction with a  $Q$ -factor  $Q = 7.24 \times 10^5$  and a mode volume  $V_{eff} = 0.3(\lambda/n)^3$ . At the conference, more simulation results for defects located at other positions (including  $1.5*L$  and  $2*L$ ) will be reported.

**ACKNOWLEDGMENT**

This work was carried out using the computational facilities of the Advanced Computing Research Centre, University of Bristol, Bristol, U.K. We acknowledge financial supports from the ERC advanced grant 247462 QUOWSS, the EU FP7 grants 618078 WASPS, and EPSRC grant EP/M009033/1.

**REFERENCES**

- [1] J. D. Joannopoulos et al., *Photonic Crystals: Molding the Flow of Light*, 2<sup>nd</sup> ed., Princeton Univ. Press, 2008.
- [2] G. von Freymann et al., *Adv. Funct. Mater.*, vol. 20, pp.1038, 2010.
- [3] L. Chen et al., “First evidence of near-infrared partial photonic bandgap in polymeric rod-connected diamond structure,” arXiv:1501.03741v2, 2015.
- [4] C. Chan et al., *Phys. Rev. B*, vol. 50, pp. 1988, 1994.
- [5] M. Maldovan et al., *Nat. Mater.*, vol. 3, 593, 2004.
- [6] H. Men et al., *Opt. Express*, vol. 224, pp.17, 2014.
- [7] S. G. Johnson et al., *Opt. Express*, vol. 8, pp. 173, 2001.
- [8] S. Imagawa et al., *Appl. Phys. Lett.*, vol. 100, pp. 151103-151104, 2012.
- [9] S. G. Johnson et al., *Opt. Express*, vol. 8, pp.173-190, 2001.
- [10] C. Raitlon et al., vol. 47, pp. 707-714, 1999.
- [11] M. P. C. Taverne et al., *J. Opt. Soc. Am. B*, 32, pp. 639-648, 2015.
- [12] K. J. Vahala, *Nature*, vol. 424, pp. 839-846, 2003.